OPEN ACCESS Freely available online

Journal of Geology & Geophysics

ISSN: 2381-8719

Research Article

Prediction of Water Saturation Applying the Extended Elastic Impedance Inversion, Offshore Nile Delta, Egypt

Adel A A Othman[1], Mohamed Fathi Mohamed Ali[1], Ahmed Saied Ali[2*], Farouk Ibrahim Metwally[3]

[1]Geology Department, Al-Azhar University, Nasr City, Cairo, Egypt; [2]Qarun Petroleum Company, New Maadi, Cairo, Egypt; [3]Geology Department, Helwan University, Cairo, Egypt

ABSTRACT

Extended Elastic Impedance (EEI) is very useful seismic reconnaissance attribute. EEI logs can be directly corresponds to the petro physical properties of the reservoir and the seismic. EEI reflectivity volumes can be obtained directly from the pre-stack seismic data. A better discrimination between the seismic anomaly caused by either lithology or fluid content can be utilized applying this approach.

The concept of extended elastic impedance is used to derive the petro physical properties and distribute the reservoir facies. The study area was a Pliocene gas field that lies in the deep marine, Offshore Nile Delta, Egypt. The workflow is simple, efficient and uses very few inputs. We started with the fluid/lithology logs and investigated the optimum projection in the intercept/gradient domain. Then, we used the conditioned angle stacks, to calculate the intercept/gradient volumes, using Shuey's two terms Approximation. The intercept and gradient volumes are converted directly to the fluid and lithology 3D volumes, without any of the pre-stack inversion's constrains. The outputs were tested using a blind well and the correlation exceeds 80%. The results show that the EEI is a worthy effort to highlight the difference between the reservoir and non-reservoir sections, to identify the hydrocarbon area.

Keywords: Extended elastic impedance; Seismic inversion; water saturation; Saffron field; Nile delta

INTRODUCTION

The area of interest includes Saffron field, which lies in the West Delta Deep Marine (WDDM) concession, 60–120 km offshore in the deep water of the present-day Nile Delta (Figure 1). Saffron field is a Pliocene submarine delta slope canyon system, with complex turbiditic channel-levee reservoirs [1].

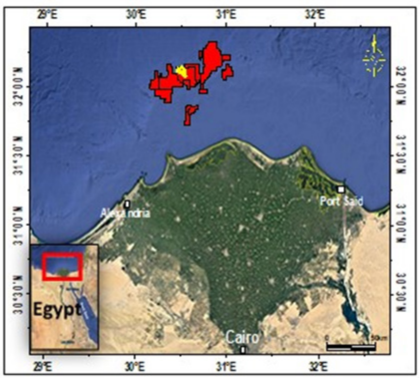

Figure 1: Location map of the Saffron field (in yellow) in the West Delta Deep Marine Concession WDDM (in red) (modified from Google Earth).

The Nile Delta lies within the unstable shelf, which is characterized by a thick sedimentary section covering the high basement relief due to block faulting. It is affected by minor compression folds trending (NNE-SSW) which is related to the Laramide phase of the Alpine Orogeny. The sedimentary succession of the Nile Delta is characterized by the cyclicity that began in the Miocene time with a very thick section of Late Tertiary-Quaternary sediments indicating a rapid and continuous deposition in a subsiding basin. This section consists mainly of shale with thin sandstone intercalations (Figure 2).

Saffron field was discovered by the Saffron-1 exploration well in 1998 by BG and appraised by Saffron-2.

The reservoir consists of a succession of sandstones and mudstones, organized into a composite upward-fining profile. Sand bodies include laterally amalgamated channels, sinuous channels, channels with frontal splays and leveed channels, and are interpreted to be the products of deep-water gravity-flow processes (Cross et al.). The Saffron channel system is oriented

Correspondence to: Ahmed Saied Ali, Qarun Petroleum Company, New Maadi, Cairo, Egypt, Tel: +201009695999; E-mail: Aali_13@hotmail.com

Received: March 1, 2021, **Accepted:** March 15, 2021, **Published:** March 22, 2021

Citation: Othman AAA, Ali MFM, Ali AS, Metwally FI (2021) Prediction of Water Saturation Applying the Extended Elastic Impedance Inversion, Offshore Nile Delta, Egypt. J Geol Geophys. 10:983.

NNW-SSE to N W-SE (Figure 3) and its width ranges from 5 km to 10 km, and is approximately 25 km in length. There is almost 40 m of pay gas sand, out of 150 m gross thickness of the reservoir, with an average porosity of 25% and an average Sw of 37% [2-5].

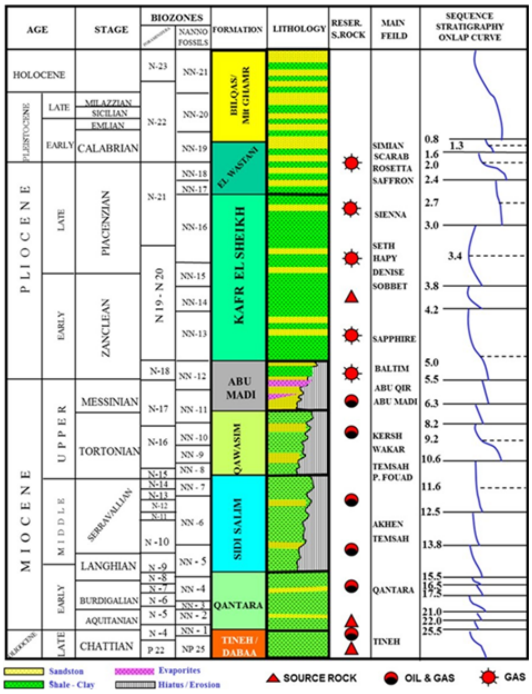

Figure 2: Stratigraphic succession of the Nile Delta and the hydrocarbon system for the main fields modified.

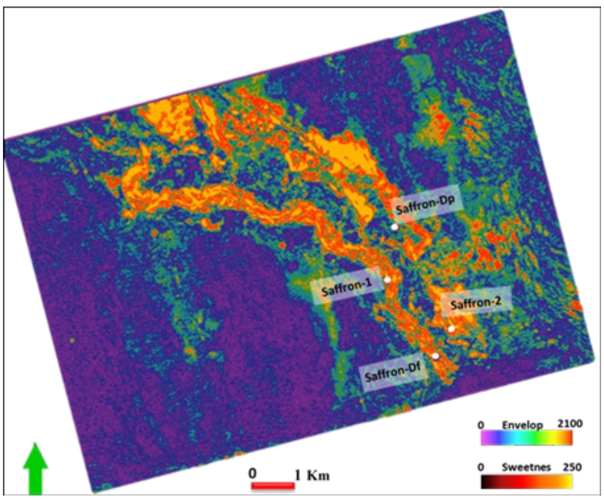

Figure 2: Reflector strength attribute extracted below the top of the channel and illustrates the orientation of the channel and the available well data.

METHODOLOGY

The available data are classified into well logs and pre-stack 3D seismic volume data. The obtained well logs include Gamma-Ray(GR), Resistivity(Rt), P-wave velocity(VP), S-wave velocity vs. density(ρ) logs, in addition to the calculated Petro physical logs which are water saturation (Sw), and shale volume (V_{shale}) logs. Three wells will be involved in this study, and another one will be used as blind QC well. Figure 4 illustrates an example of our data.

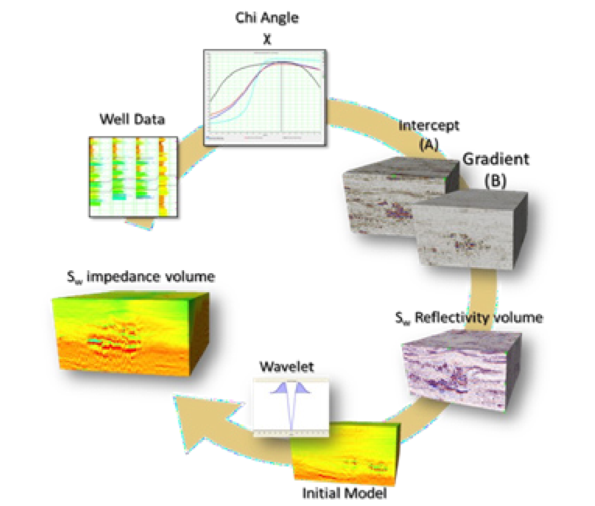

Figure 4: Extended elastic impedance workflow.

The Workflow for the Extended Elastic Impedance (EEI) is shown in Figure 3. The first step is to load and QC input 3D seismic data and water saturation logs then perform EEI log correlation at each well in order to determine the best chi angle at which we got an optimal correlation of EEI log and the Sw log. Figure 4 shows that the high correlation for Sw is associated with approximately specific chi for all wells and the average [6].

Correlation is 80% observed at a chi angle of approximately 28°. Conditioning the seismic data should be applied carefully, in order to give a meaningful result. After conditioning, first, we created the intercept and gradient volumes, applying the two-term Aki-Richard approximation, because there is no wide-angle range. Second, we created a reflectivity volume at the chi angle that obtained previously from the well data, through applying the following equation:

$Rs=A \cos x+B \sin x$

Where, Rs is the scaled reflectivity, A is the intercept, B is the gradient and *x*: is the chi angle.

Third, we estimated the wavelet from the created reflectivity volume, before creating the synthetic trace, in order to make a well-to-seismic tie at the optimized chi angle, with the corresponding trace at the reflectivity volume, which is considered as a good measure of the wavelet and chi angle estimations. Then, we built an initial model, using the EEI logs created at angle 28° in order to invert that volume, to get a 3D cube for the water saturation property distribution for the reservoir [7,8].

RESULTS AND DISCUSSION

Simultaneous seismic inversion and extended elastic impedance (EEI) were applied to obtain quantitative estimates of porosity, water saturation, and shale volume over Nianga field of Congo basin, West Africa. The optimum angle at which EEI log and the target petrophysical parameter give the maximum correlation was meticulously analyzed by additionally incorporating the concept of relative rock physics. Prestack seismic data were simultaneously inverted into Vp, acoustic, and gradient impedances. The last two broadband inverted volumes were projected to Chi angles corresponding to the target petrophysical parameters, and three broadband EEI volumes were obtained. At well control points, the linear trends based on specific lithology between EEI and petrophysical parameters were then used to transform EEI volumes into quantitative porosity, water saturation, and shale volume cubes. In order to obtain the reservoir facies distribution, another concept of minimum energy angle was used to generate the background EEI cube, thereby enabling the mapping of reservoir facies. From quantitative porosity, water saturation, shale content, and background EEI cubes, favorable zones have been pinpointed which may suggest possible drilling locations for future development of the field.

The aim of this study is to discriminate reservoir from non-reservoir facies of the Ghar formation in one Iranian oil field within the Persian Gulf, using extended elastic impedance (EEI) inversion. The Ghar reservoir, as a member of the Asmari Formation, consists of reservoir unites with interbedded shales. It is often difficult to separate these units. The lithological facies discrimination of the Ghar reservoir was applied, using the simultaneous application of EEI attributes. The EEI inversion method used best . Angles from cross-correlation based on a model-based inversion algorithm to generate the EEI attributes. In the facies discrimination, the lithological facies volume was provided based on EEI Lambda-Rho versus EEI Mu-Rho cross-plot mapping together with porosity, water saturation, shale volume, sand volume and dolomite volume, which attributes indicated good definition of the reservoir unites with low values. The volume of the facies discrimination presented excellent separation of lithological facies, consistent with the well logs with petro-physical interpretations. As a result of this study, three facies in several stratigraphic levels of the Ghar reservoir were identified: sandstone facies, dolomite-sandstone facies (tight and porous), and shaly facies. As a result, the middle part of the Ghar reservoir was identified as the most porous reservoir unite, consistent with lower EEI Lambda-Rho and EEI Mu-Rho values. Since all the well locations were drilled in the southern part of this field, the results can be practical for well location drilling and field development in the northern part of the field.

For QC purposes, we kept one well away in our study, in order to use it as a QC well for the results. The blind well is Saffron-Df, which lies to the south of the study area. The correlation coefficient between the actual Sw log and the calculated water saturation is 0.71, we compared the results of the 3D water saturation volume at the blind well location, as can be seen in Figures 5-7 where the distribution of the saturation will give an insight to the charged sand bodies [9,10].

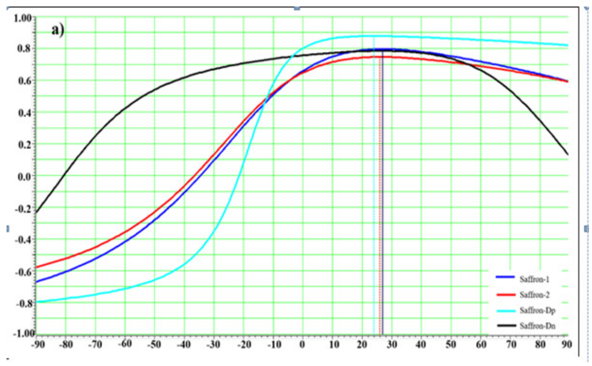

Figure 5: Illustrates the correlation coefficients between the Sw curve and EEI log, for a range of values of , the highest correlation occurs at =28°, is 88% at Saffron-Dp, while the lowest correlation is 72% at Saffron-2, and 80% and 75 % at Saffron-1 and saffron-Dn, respectively.

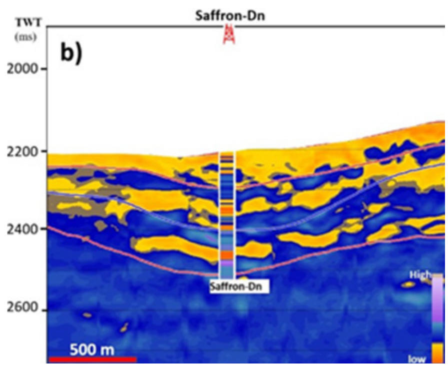

Figure 6: Seismic section passing through the resulted EEI at =28° volume of (Sw), as comparing its results to the calculated Sw log at the blind well.

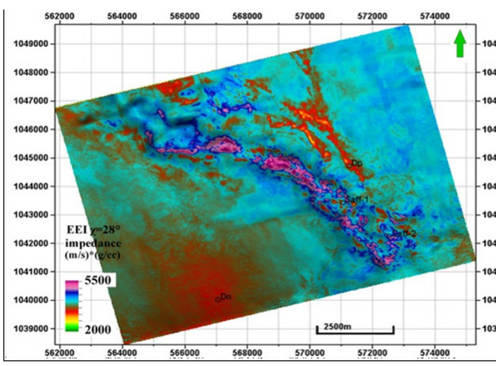

Figure 7: Minimum amplitude extraction on reservoir zone on Sw impedance volume showing the distribution of the gas saturation.

CONCLUSION

Saffron field has a complex largely channelized fill, with multiple phases of re-incision, and was probably active over a considerable period. The Extended Elastic Impedance (EEI) has successfully predicted the 3D volume of water saturation, which is considered as one of the required elements for reservoir modeling. The EEI workflow was straightforward and non-complicated, which starts with identifying the Chi angle that corresponds to the water saturation, in order to produce reflectivity volume of the property. The last step is to invert the latter volume into the required petro physical property (Sw). Results show a good correlation to the actual saturation, which encourage to be applied on the same slope channel systems of clastic reservoirs.

REFERENCES

1. Mohamed I A, Shenkar O, Mahmoud H. Understanding reservoir heterogeneity through water-saturation prediction via neural network : A case study from offshore Nile Delta. Lead Edge. 2017;36:298–303.
2. Cross NE, Cunningham A, Cook RJ, Taha A, Esmaie E, Swidan N EL. Three- dimensional seismic geomorphology of a deep-water slope-channel system: The Sequoia field, offshore west Nile Delta, Egypt. Am Assoc Pet Geol Bull. 2009;93:1063–1086.
3. Rio D, Sprovieri R, Thunell R. Pliocene-lower pleistocene chronostratigraphy: A re-evaluation of Mediterranean type sections. Geol. Soc. Am. Bull. 1991;93:1049–1058.
4. Hrouda F. Magnetic anisotropy of rocks and its application in geology and geophysics. Surv Geophys. 1982;5:37-82.
5. Goldberg D. The role of downhole measurements in marine geology and geophysics. Rev. Geophys. 1997;35:315-342.
6. Turcotte DL. Fractals in geology and geophysics. Pure Appl Geophys.1989;131:171-196.
7. Shephard GE, Müller RD, Seton M. The tectonic evolution of the Arctic since pangea breakup: Integrating constraints from surface geology and geophysics with mantle structure. Earth-Sci. Rev. 2013;124:148-183.
8. Hauber E, Grott M, Kronberg P. Structural geology and geophysics. Earth Planet Sci Lett. 2010;294:393-410.
9. Solomon SC, Head JW. Fundamental issues in the geology and geophysics of Venus. Sci. 1991;252:252-260.
10. Turcotte DL, Newman WI. Symmetries in geology and geophysics. Proc. Natl. Acad. Sci. 1996;93:14295-14300.